Abiotic Hydrocarbons Discharge from A Felsic Rock-Hosted Hydrothermal System

Xue-Gang Chen [1, *], Ming-Zhen Yu [1, 2], Mark Schmidt [3], Pei Sun Loh [1], Shuhei Ono [4], Chen-Tung Arthur Chen [5], Ying Ye [1]

1 Ocean College, Zhejiang University, Zhoushan 316021, China

2 Department of Earth and Planetary Sciences, Harvard University, Cambridge, MA02138, USA

3 GEOMAR Helmholtz Center for Ocean Research Kiel, 24148 Kiel, Germany

4 Department of Earth, Atmosphere, and Planetary Sciences, Massachusetts Institute of Technology, Cambridge, MA 02139, USA

5 Department of Oceanography, National Sun Yat-sun University, Kaohsiung 80424, Taiwan

To whom correspondence should be addressed: Xue-Gang Chen, Email: chenxg83@zju.edu.cn. Tel: +86-580-2092326; Fax: +86-580-2092891; **ORCID**: 0000-0002-9148-8309

Abstract

Abiogenic hydrocarbons are fundamentally important for understanding the deep microbial communities and the origin of life. The generation of abiogenic hydrocarbons was proposed to be limited to ultramafic-hosted hydrothermal systems, fueled by the serpentinization product H_2. Here, we present the discharge of short-chain alkanes from an andesitic rock-hosted Lutao geothermal field in the north Luzon arc, carrying abiotic chemical

and isotopic signals. These abiogenic hydrocarbons were generated from CO_2-H_2O-rich fluid inclusions, where the long-term storage since Lutao volcanism (~ 1.3 Ma) allowed overcoming the sluggish kinetics of CO_2 to CH_4 reduction at temperatures of 174 - 206 ºC. Natural abiogenic production of hydrocarbons, therefore, can be more ubiquitous than previously thought. The hypothesis regarding the origin of methane in Earth's early atmosphere and its implication to the origin of life may require reconsideration.

Keywords: abiotic; hydrothermal; methane; clumped isotope

Introduction

Methane and other light hydrocarbons within Earth's interior are generated by either abiotic or biotic pathways. Studying the origin of abiotic hydrocarbons is especially crucial for diverse topics such as the global carbon cycle and the origin of life [1–3]. In natural settings, Fischer-Tropsch type (FTT) reaction is one of the most profound processes to produce abiotic hydrocarbons in hydrothermal/geothermal systems [4]. It requires H_2 as a reactant, which is usually provided by the serpentinization of ultramafic rocks with abundant olivine or pyroxene [5]. However, laboratory studies indicated that the production rate of abiogenic hydrocarbons highly relies on catalysts such as transition metals and chromite [6,7]. Multiple pieces of evidence suggested that naturally abiogenic formation of methane from FTT reactions were sluggish [8,9]. An alternative process is that the formation of abiogenic hydrocarbons was disconnected with active hydrothermal circulation. Abiotic methane was mostly released from methane-rich inclusions, which were generated from the respeciation of C-O-H fluids during magma cooling [10]. This process has been suggested to be responsible for

the abiotic methane released from the ultramafic-hosted Rainbow, Lost City, and Von Damm hydrothermal fields [11,12]. A recent study further testified that abiotic methane formation in olivine-hosted inclusions is a widespread process [13].

Results and Discussion

Abiogenic hydrocarbons released from an andesite-hosted hydrothermal system

Nevertheless, no matter the abiogenic hydrocarbons were produced from FTT reaction during hydrothermal circulation or fluid inclusions disconnected with circulation, ultramafic rocks or serpentinization were recognized as a key role in the formation of abiogenic hydrocarbons [14]. Here, we present geochemical evidence for abiotic hydrocarbons discharging from hot springs of the andesitic rock hosted sediment starved Lutao geothermal system. Lutao is a volcanic island tectonically belongs to the Luzon volcanic arc (Supplementary Fig. S1). N_2 and CH_4 dominated the discharged bubbling gas, showing concentrations of 806-837 and 96-172 mmol/mol, respectively (Supplementary Table S1 and S2). When we plot the $\log_{10}(C_n/n)$ against the carbon number (n), which is called the Anderson-Schulz-Flory (ASF) plot, it displays a near linear trend with a chain growth probability α of 0.1 at n=3-5 (Fig. 1). This trend is produced by either the polymerization of kinetically controlled FTT reactions or random breakage of thermogenic hydrocarbons [15]. The Lutao hydrocarbons showed relatively higher C_1 but lower C_2 values than that predicted by the linear ASF plot. It may be ascribed to the molecular fractionation that commonly occurred for surface gas seeps [16]. Alternatively, it is also a common result of kinetically controlled polymerization that has been reported in the field of chemical engineering [17]. The

relationships among hydrocarbons all show strong linear correlations with $R^2 > 0.9$ (Supplementary Fig. S2). It is suggested that these hydrocarbons may originate from the same source without significant secondary alterations during hydrothermal circulation, including microbial oxidation, gas diffusion, or mixing between different sources.

Thermogenic hydrocarbons, produced from the thermal cracking of organic matter, commonly display δ^{13}C-CH_4 values of -50 to -20‰ (VPDB), while microbial methane usually show δ^{13}C values < -40‰ [18]. The Lutao δ^{13}C values of CH_4 fall in a range between -17.8 and -6.7‰ (Fig. 2), which is comparable to proposed abiogenic CH_4 from ultramafic-hosted Rainbow and Lost city hydrothermal systems [14,19]. Abiogenic or microbial oxidation of CH_4 would significantly increase the δ^{13}C values of residual CH_4 [20,21]. In the Lutao gas, however, CO_2 was in trace amount mostly less than 10 mmol/mol; the δ^{13}C values of CO_2 were mostly lighter than -13‰, which is significantly lighter than magmatic CO_2 (-4 ~ -7‰ VPDB) [22]. It is suggested that the magmatic CO_2 that commonly found in other hydrothermal systems has been dissolved or removed before venting. At a pH of 7.8 and temperature of 90°C, the fractional dissolution will dissolve about 60% CO_2 into the fluid phase and 40% remain in the gas phase. The δ^{13}C fractionation between gaseous CO_2 and dissolved carbonate would be ~ -1.8‰ [23]. Therefore, the fractional dissolution and isotopic fractionation are not the main factors to produce the low content and light δ^{13}C values of Lutao CO_2. Consequently, the Lutao CO_2 was mainly contributed by the oxidation of, i.e., hydrocarbons (mainly CH_4). It is confirmed by the increasing δ^{13}C(CH_4) values with CO_2/CH_4 ratios (Supplementary Fig. S3), where the variations fit well with the modeled

results of methane oxidation using a fractionation factor ΔCO_2-CH_4 of -15 ~ -35‰ [18]. The estimated endmember $\delta^{13}C$ and $\delta^{2}H$ values of CH_4 were -19 to -15.5 ‰ VPDB and -90 to -75‰ VSMOW, respectively, both of which fall in the typical range of abiogenic methane. Most samples showed low CH_4-CO_2 conversion ratio of <10%.

Another compelling evidence for the abiogenic origin of Lutao hydrocarbons is the isotope reversal of $\delta^{13}C$ values (Table 1 and Fig. 2). The $\delta^{13}C$ values of thermogenic hydrocarbons usually become increasingly enriched in ^{13}C with increasing chain length because the decomposition of organic matter preferentially at ^{12}C-^{12}C bonds with weaker bond strength than ^{12}C-^{13}C bonds. A reversed isotopic trend ($\delta^{13}C_1 > \delta^{13}C_2 > \delta^{13}C_3$) is a plausible indicator of abiogenic hydrocarbons [14,24]. The isotope reversal of abiogenic hydrocarbons has been observed in the Murchison meteorite and Kidd Creek, Precambrian shield [25,26], and also during the sparking experiment in a methane atmosphere [27]. Although gas diffusive migration or mixing between thermogenic gases with different sources or thermal maturities may also create an isotopic reversal of $\delta^{13}C$ values [28,29], the $\delta^{13}C(CH_4)$ values (< -25‰) of these gases all fall in the range of typical thermogenic CH_4. The δD values of Lutao hydrocarbons show a similar inversed trend that decreased from -55~-90‰ of CH_4 to -60~-185‰ of C_2H_6 and -163 ~ -168‰ of C_3H_8 (Supplementary Fig. S4). This trend is like the abiogenic hydrocarbons occurred in the Lost City hydrothermal system [14] and produced in a closed-system FTT synthesis [30]. Furthermore, if we plot the δD values of Lutao hydrocarbons against their $\delta^{13}C$ values (Supplementary Fig. S5), it displays a pattern that falls outside of the range of typical biotic hydrocarbons [16]. An increasing maturity, gas diffusion,

or hydrocarbon oxidation may increase both the $\delta^{13}C$ and δD values of residual hydrocarbons. However, the significant influence of these secondary processes has been precluded by the linear ASF distributions and the CO_2-CH_4 conversion ratio of <10%. Two Lutao samples, which showed considerably heavier $\delta^{13}C$ and δD values of CH_4 than other samples, may have experienced significant (microbial) methane oxidation ($\Delta H/\Delta C$=8.6, Supplementary Fig. S3) with respect to other samples [31]. All the other samples with original $\delta^{13}C(CH_4)$ of -19 ~ -15.5‰ are hard to be explained as a product of microbial oxidation.

Disconnection with hydrotermal circulation

Abiogenic hydrocarbons could be produced from mantle and magmatic processes, aqueous CO_2 reduction and FTT reactions during hydrothermal circulation, or fluid inclusions [8,16]. The calculated fO_2 of andesite in North Luzon arc eliminated the possibility of methane directly originated from the mantle/magma, where the C-O-H fluids should be dominated by CO_2 and H_2O (Supplementary T2). Both aqueous CO_2 reduction and FTT reactions during hydrothermal circulation require H_2 as a reactant [7,16] but H_2 was below detection limit in most Lutao samples. It implies that either Lutao hydrocarbons were not produced from the H_2-involved CO_2 reduction or FTT reaction, or H_2 has been removed after these reactions, e.g., by microbial consumption [18,32]. Even the only sample showing H_2 content of 0.99 ‰ was possibly a result of microbial production of hydrogen. In addition, experimental studies suggested that abiogenic production of hydrocarbon by FTT reactions would be sluggish without catalysts such as chromite, magnetite, and FeNi [6,8,33]. Again, there is no evidence for such catalysts in the Lutao intermediate rock. Therefore, it is hard to

conclude that the Lutao hydrocarbons were generated from the FTT reactions during active hydrothermal circulation.

The radiocarbon test on the methane in two Lutao samples indicated that both samples present ^{14}C contents of below detection limit (fraction of modern carbon <0.0044, or age > 43500 BP) (Table 2). Consequently, the carbon source cannot be the modern seawater carbonate that is actively circulating the Lutao geothermal system, neither the radiocarbon-rich Holocene-elevated coral reef that covers the geothermal field [34]. This result again indicated that the formation of Lutao hydrocarbons was disconnected from active hydrothermal circulation.

Potential source from fluid inclusions

Alternatively, the Lutao short-chain alkanes may have been leached from fluid inclusions of plutonic rocks. During the Lutao volcanism at 1.3 Ma, magmatic C-O-H fluids (dominated by CO_2 and H_2O) were trapped in the intrusive rocks, which later achieved equilibrium (the equilibration may take over geological time scale to overcome the sluggish kinetic barrier) with geothermal gradients and formed alkane-rich inclusions (Supplementary Fig. S6). Under such circumstance, (1) the formation temperature of methane should be identical to the temperature of C-O-H fluids at equilibrium as well as that of water/rock reaction. This is the case for the Lutao methane which was formed at 174 – 206°C (Table 2) calculated from the methane isotopologue ($\Delta^{13}CH_3D$) abundance. This temperature range is close to the temperature of CO_2-CH_4 pair (180 – 206°C, Fig. 3) when achieving both chemical and isotopic equilibriums [15,35], and similar to the temperature of W/R reaction (150

– 175°C) estimated from the Si-geothermometer. The δ^2H values of Lutao methane were -80 ~ -90‰, also match that predicted by the D/H fractionation model with an initial magmatic H_2O/CO_2 ratio of 2 (Supplementary Fig. S7). All these results suggested that the C-O-H fluids have reached both chemical and isotopic equilibrium with temperature gradient in a closed environment. This hypothesis also works for the methane released from the other low-temperature vapor spring (the HWC vent) at Lutao field, although whether the HWC methane has experienced anaerobic oxidation is still uncertain (Supplementary T4).(2) If Lutao hydrocarbons were leached from the fluid inclusions in the host rock, then both the crustal component for the Lutao helium and the CH_4 abundance will increase with enhanced W/R reaction. The measured $CH_4/^3He$ ratios of Lutao gas samples decreased linearly with R/Ra values (i.e., increasing of crustal contributions) (Fig. 4), further testified the hypothesis that Lutao abiogenic methane was released from fluid inclusions. A rough estimation suggested that the annual methane flux is about 1000 – 1500 m^3, which only consumes 8.1 ~ 9.6*10^{-4} km^3 host rock (Supplementary T5). Therefore, the Lutao host rock could sustain the continuous releasing of abiotic methane.

Similar processes have been reported in the Von Damm field, the SWIR, Rainbow, and Lost City hydrothermal systems [10–13]. These fields, however, mostly associated with ultramafic/alkaline rocks or significant serpentinization, where H_2 with abundant concentrations played a vital role in the formation of methane. The Lutao andesite and its plutonic diorite, on the contrary, are dominated by felsic minerals (plagioclase and amphibole). The average olivine content is about 1.4% and the FeO content fall in a range of

4% ~ 9% (Supplementary T1). Based on thermodynamic calculations (Supplementary T6), the Lutao methane may be produced from a one-step respeciation of C-O-H fluids (equation 1), or a two-step process started with serpentinization of olivine and pyroxene at the initial stage of magma cooling to <400 ^{o}C (equation 2) and followed by Sabatier reaction (equation 3). However, massive serpentinization is questionable due to the small amount of both olivine and pyroxene. Fe(II)-bearing minerals with FeO content of 4% ~ 9% in the Lutao host rock [36] may have provided a redox environment to make these reactions thermodynamically more favorable. In addition, although these reactions are kinetically sluggish without proper catalysts [8,9], the long-term processing (over geological time scale) may have helped to overcome this kinetic barrier and make the C-O-H fluids in the inclusions to achieve equilibrium. H_2 was not produced from the one-step reaction and could have been largely consumed if methane was formed through the two-step mechanism [10,13]. Therefore, H_2 was almost absent in the Lutao gas samples.

$$12FeO + CO_2 + 2H_2O = CH_4 + 4Fe_3O_4 \quad (1)$$

$$6FeO + 2H_2O = 2H_2 + 2Fe_3O_4 \quad (2)$$

$$CO_2 + 4H_2 = CH_4 + 2H_2O \quad (3)$$

Implications

Lutao field may be one of many but yet undiscovered felsic rock-hosted hydrothermal systems that discharge abiogenic hydrocarbons. For instance, the methane released from arc volcanic hydrothermal systems at the Mediterranean and continental serpentinized fields (Chimaera and Zambales Ophiolite) well follows the hypothesis that methane was produced

from CO_2 in a closed system, i.e. in fluid inclusions (Fig. 3, Supplementary Fig. S7). The measured $\delta^{13}C$- and δD-methane values may represent hydrocarbon-rich inclusions equilibrated at different temperatures <200°C. Methane discharged from Mid-Ocean Ridge (MOR) type hydrothermal systems, however, does not fit our proposed model (Supplementary Fig. S8), and hydrogen isotope ratios of methane are possibly ascribed to the fast D/H exchange between equilibrated CH_4 and vent fluids during fluid migration and venting [12].

Our findings suggest that abiogenic production of hydrocarbons in host rocks should be a globally ubiquitous process rather than previously thought to be limited to ultramafic-hosted/serpentinized fields, providing that magmatic C-O-H fluids have been trapped into Fe(II)-bearing intrusive rocks during volcanism. This process is fundamentally important for methane-related studies such as methane supply for deep microbial ecosystem, Earth's carbon cycle, and source of methane in Earth's early atmosphere as well as the origin of Martian methane.

Methods

Sampling

We conducted five sampling campaigns in May 2012, Apr 2014, Sep 2014, May 2016, and Oct 2018, respectively. During the previous three sampling campaigns, the bubbling gas was collected by self-made piston gas samplers with an inner diameter of 40 mm, a length of 145 mm, and a volume of 182 mL. The sampler was firstly filled by vent fluids and was then turned upside down and immersed in a container filled with vent fluids. The bubbles

discharged from the hot spring were collected using a glass funnel connected to a silicon tube by the displacement of water. The sampler was sealed by a gas-tight cap after the gas sampling. Potential contamination during hot gas sampling was precluded by using Teflon as the materials of the whole sampler, pre-cleaning by HNO_3, and absent using of lubricating grease.

In May 2016 and Oct 2018, the gas samples were collected by low-permeability glass bottles with a volume of about 100 mL. The sampling procedure was identical to that conducted in 2012 and 2014. After the sampler was filled with bubbling gas, the sampler was sealed by a butyl rubber stopper and an aluminum seal. After sampling, several selected samples were sterilized by adding 1 mL 1% $HgCl_2$ solutions, in order to study the effect of microbial oxidation on the chemical and isotopic compositions of hydrocarbons.

Analyzing methods

The gas compositions of non-hydrocarbons were measured at the Key Laboratory of Petroleum Resources Research, Institute of Geology and Geophysics, Chinese Academy of Science (CAS) by a MAT 271 (Finnigan, USA) mass spectrometer (MS). The operating conditions were: ionization energy of 86 eV, emission current of 40 mA, ion source temperature of 95 ^{o}C, injection volume of 1 mL, and scanning using selected ion monitoring. The detection limit for all gas species was 0.001 mmol/mol. The precision of this analysis was about 3%.

For the 2012-2014 samples, the low-molecular-weight hydrocarbon abundances were determined in CAS using a GC-9160 (Shanghai Ouhua, China) gas chromatograph (GC), equipped with one thermal conductivity detector (TCD) and two flame ionization detectors (FID). The temperature programming was: 35 ^{o}C for 5 min, and 10 min at 200 ^{o}C, with a temperature increase of 10 ^{o}C min^{-1}. The overall precision is about 5%. The hydrocarbon concentrations of the 2016 samples were measured in Helmholtz-Zentrum für Ozeanforschung Kiel (GEOMAR) using a Shimadzu gas chromatograph (GC2014) equipped with flame ionization detector and thermal conductivity detector, and a HayeSepTM Q 80/100 column with a length of 2 m and diameter of 1/8''. A precision of ±2-10% was achieved when measuring standard hydrocarbon mixtures and synthetic air.

The isotopes of He and Ne of all samples were analyzed in CAS by an MM5400 mass spectrometer (Micromass, UK). The voltage and emission current were kept at 9.0 kV and 800 mA, respectively. The air from the top of GaoLan Mountain (Lanzhou, China) was chosen as the reference material to check the accuracy and precision of the analyses. The helium isotopic characteristics (R = ^{3}He/^{4}He) were corrected by assuming that all ^{20}Ne was originated from air contamination. The equation is expressed as follows [37]:

$$R_c = (R_m - R_a{*}r)/(1 - r) \quad (4)$$

$$r = (^{4}\mathrm{He}/^{20}\mathrm{Ne})_a/(^{4}\mathrm{He}/^{20}\mathrm{Ne})_m \quad (5)$$

where the subscripts c, m, and a denote the corrected value, measured value, and air value, respectively.

The stable carbon isotopic compositions ($\delta^{13}C$) of the 2012-2014 samples were determined in CAS by a DeltaPlus XP mass spectrometer (Thermo Fisher Scientific, USA). The carbon species were separated by a Carbobond chromatographic column (30 m * 0.53 mm * 20 μm) following the temperature program: 50 ºC for 5 min and 15 min at 200 ºC, with a temperature increase of 20 ºC min^{-1}. The separated gases were oxidized to CO_2 by CuO at 900 ºC and were then analyzed for $\delta^{13}C$ values. The 2016 samples were analyzed in GEOMAR by using continuous flow GC combustion - Isotope Ratio Mass Spectrometry. Single gas components were separated in a Thermo Trace GC with a packed Shin Carbon Column using He as the carrier gas. The subsequent conversion of hydrocarbons to CO_2 was conducted in a Ni/Pt combustion furnace at 1150 °C. The $^{13}C/^{12}C$-ratio of produced CO_2 was determined by a Thermo MAT253 isotope ratio mass spectrometer. The results were reported with respect to Vienna Pee Dee Belemnite (vPDB), and the measurement uncertainties calculated from duplicate analyses of the samples and reference materials were less than 0.5‰.

The deuterium isotope ($\delta^{2}H$) of the 2012-2014 samples was also analyzed in CAS using a MAT253 (Finnigan, USA) mass spectrometer. The low-molecular-weight hydrocarbons were separated by an Al_2O_3 chromatographic column (50 m * 0.53 mm * 20 μm) with an initial temperature of 45 ºC for 5 min and 200 ºC for 5 min at a heating rate of 25 ºC min^{-1}. The separated gas was transformed to H_2 by a ceramic reaction tube at 1450 ºC. Then the generated H_2 was analyzed for $\delta^{2}H$ values, which was reported with respect to Vienna - Standard Mean Ocean Water (vSMOW). The measurement uncertainties were less than 10‰.

The 2016 samples were analyzed by GEO-data GmbH (Garbsen, Germany) using a continuous flow isotope ratio analysis method. The hydrocarbons were separated by a Hewlett-Packard HP 9890 Series II equipped with a 10 m long 16" SS- tube filled with Shin Carbon. Temperature program: 70 °C/ hold 5 min, heat to 320 °C at a rate of 22 °C per min and hold 20 min. The separated hydrocarbons were reduced to H_2 and C in an empty ceramic tube at 1300 °C. The gas cleaning was carried out with Molsieve 5A. The cleaned H_2 was transferred into the mass spectrometer (CF-IRMS, PDZ EUROPA 2020) with a long-spur fly tube via an open split interface. The reproducibility of the δ^2H values was about ± 2‰.

The $\delta^{13}C$, δ^2H, and methane isotopologue abundances ($\Delta^{13}CH_3D$) of the 2018 samples were measured in the stable isotope laboratory of Massachusetts Institute of Technology, using a tunable infrared laser direct absorption spectroscopy, following the methods of [38,39]. The measurement uncertainties for $\delta^{13}C$ and δ^2H were ± 0.2‰ and ± 0.1‰, respectively.

The radiocarbon activity of methane in two selected samples was determined by an Accelerator Mass Spectrometry in Beta Analytic Inc. (Miami, USA). The measurements were conducted according to ISO/IEC 17025: 2005 Testing accreditation PJLA#59423 standards. The reported values were calculated relative to NIST SRM-4990B and corrected for isotopic fractionation. The results are reported using the direct analytical measured fraction modern (*Fm*) with one relative standard deviation.

Data availability

The data sets in this study are available as Supplementary Information and from the corresponding authors.

References

1. Martin, W., Baross, J., Kelley, D. & Russell, M. J. Hydrothermal vents and the origin of life. *Nat. Rev. Microbiol.* **6**, 805–814 (2008).
2. Schrenk, M. O., Brazelton, W. J. & Lang, S. Q. Serpentinization, carbon, and deep life. *Rev. Mineral. Geochem.* **75**, 575–606 (2013).
3. Dodd, M. S. *et al*. Evidence for early life in Earth's oldest hydrothermal vent precipitates. *Nature* **543**, 60–64 (2017).
4. Bradley, A. S. & Summons, R. E. Multiple origins of methane at the Lost City Hydrothermal Field. *Earth Planet. Sci. Lett.* **297**, 34–41 (2010).
5. McCollom, T. M. & Seewald, J. S. Abiotic synthesis of organic compounds in deep-sea hydrothermal environments. *Chem. Rev.* **107**, 382–401 (2007).
6. Foustoukos, D. I. & Seyfried, W. E. Hydrocarbons in hydrothermal vent fluids: The role of chromium-bearing catalysts. *Science* **304**, 1002–1005 (2004).
7. McCollom, T. M. Laboratory Simulations of Abiotic Hydrocarbon Formation in Earth's Deep Subsurface. *Rev. Mineral. Geochem.* **75**, 467–494 (2013).
8. Bradley, A. S. The sluggish speed of making abiotic methane. *Proc. Natl. Acad. Sci.* **113**, 13944–13946 (2016).
9. McCollom, T. M. Abiotic methane formation during experimental serpentinization of olivine. *Proc. Natl. Acad. Sci.* **113**, 13965–13970 (2016).
10. Kelley, D. S. & Fruh-Green, G. L. Abiogenic methane in deep-seated mid-ocean ridge environments: Insights from stable isotope analyses. *J. Geophys. Res.-Solid Earth* **104**, 10439–10460 (1999).
11. McDermott, J. M., Seewald, J. S., German, C. R. & Sylva, S. P. Pathways for abiotic organic synthesis at submarine hydrothermal fields. *Proc. Natl. Acad. Sci.* **112**, 7668–7672 (2015).
12. Wang, D. T., Reeves, E. P., McDermott, J. M., Seewald, J. S. & Ono, S. Clumped isotopologue constraints on the origin of methane at seafloor hot springs. *Geochim. Cosmochim. Acta* **223**, 141–158 (2018).
13. Klein, F., Grozeva, N. G. & Seewald, J. S. Abiotic methane synthesis and serpentinization in olivine-hosted fluid inclusions. *Proc. Natl. Acad. Sci.* **116**, 17666–17672 (2019).

14. Proskurowski, G. *et al.* Abiogenic hydrocarbon production at Lost City hydrothermal field. *Science* **319**, 604–607 (2008).
15. Giggenbach, W. F. Relative importance of thermodynamic and kinetic processes in governing the chemical and isotopic composition of carbon gases in high-heatflow sedimentary basins. *Geochim. Cosmochim. Acta* **61**, 3763–3785 (1997).
16. Etiope, G. & Lollar, B. S. Abiotic Methane on Earth. *Rev. Geophys.* **51**, 276–299 (2013).
17. Van Der Laan, G. P. & Beenackers, A. A. C. M. Kinetics and Selectivity of the Fischer–Tropsch Synthesis: A Literature Review. *Catal. Rev.* **41**, 255–318 (1999).
18. Whiticar, M. J. Carbon and hydrogen isotope systematics of bacterial formation and oxidation of methane. *Chem. Geol.* **161**, 291–314 (1999).
19. Charlou, J., Donval, J., Fouquet, Y., Jean-Baptiste, P. & Holm, N. Geochemistry of high H_2 and CH_4 vent fluids issuing from ultramafic rocks at the Rainbow hydrothermal field (36° 14′ N, MAR). *Chem. Geol.* **191**, 345–359 (2002).
20. Barker, J. F. & Fritz, P. Carbon isotope fractionation during microbial methane oxidation. *Nature* **293**, 289–291 (1981).
21. McCollom, T. M., Lollar, B. S., Lacrampe-Couloume, G. & Seewald, J. S. The influence of carbon source on abiotic organic synthesis and carbon isotope fractionation under hydrothermal conditions. *Geochim. Cosmochim. Acta* **74**, 2717–2740 (2010).
22. Sano, Y. & Marty, B. Origin of carbon in fumarolic gas from island arcs. *Chem. Geol.* **119**, 265–274 (1995).
23. Zhang, J., Quay, P. D. & Wilbur, D.O. Carbon isotope fractionation during gas-water exchange and dissolution of CO_2. *Geochim. Cosmochim. Acta* **59**, 107–114 (1995).
24. Fiebig, J. *et al.* Isotopic patterns of hydrothermal hydrocarbons emitted from Mediterranean volcanoes. *Chem. Geol.* **396**, 152–163 (2015).
25. George Yuen, Neal Blair, David J. Des Marais & Sherood Chang. Carbon isotope composition of low molecular weight hydrocarbons and monocarboxylic acids from Murchison meteorite. *Nature* **307**, 252–254 (1984).
26. Lollar, B. S., Westgate, T. D., Ward, J. A., Slater, G. F. & Lacrampe-Couloume, G. Abiogenic formation of alkanes in the Earth's crust as a minor source for global hydrocarbon reservoirs. *Nature* **416**, 522–524 (2002).
27. Des Marais, D. J., Donchin, J. H., Nehring, N. L. & Truesdell, A. H. Molecular carbon isotopic evidence for the origin of geothermal hydrocarbons. *Nature* **292**, 826 (1981).

28. Tilley, B. & Muehlenbachs, K. Isotope reversals and universal stages and trends of gas maturation in sealed, self-contained petroleum systems. *Chem. Geol.* **339**, 194–204 (2013).
29. Shuai, Y. *et al.* Methane clumped isotopes in the Songliao Basin (China): New insights into abiotic vs. biotic hydrocarbon formation. *Earth Planet. Sci. Lett.* **482**, 213–221 (2018).
30. Wei, Z. *et al.* Isotopic Composition of Abiogenic Gas Produced in Closed-System Fischer-Tropsch Synthesis: Implications for the Origins of the Deep Songliao Basin Gases in China. *Geofluids* **2019**, 2823803 (2019).
31. Wang, D. T., Welander, P. V. & Ono, S. Fractionation of the methane isotopologues $^{13}CH_4$, $^{12}CH_3D$, and $^{13}CH_3D$ during aerobic oxidation of methane by Methylococcus capsulatus (Bath). *Geochim. Cosmochim. Acta* **192**, 186–202 (2016).
32. Kelley, D. S. *et al.* A Serpentinite-Hosted Ecosystem: The Lost City Hydrothermal Field. *Science* **307**, 1428–1434 (2005).
33. Horita, J. & Berndt, M. E. Abiogenic methane formation and isotopic fractionation under hydrothermal conditions. *Science* **285**, 1055–1057 (1999).
34. Shen, C.-C., Wu, C.-C., Dai, C.-F. & Gong, S.-Y. Variable uplift rate through time: Holocene coral reef and neotectonics of Lutao, eastern Taiwan. *J. Asian Earth Sci.* **156**, 201–206 (2018).
35. Horita, J. Carbon isotope exchange in the system CO_2-CH_4 at elevated temperatures. *Geochim. Cosmochim. Acta* **65**, 1907–1919 (2001).
36. Chen, J. & Lin, F. Geochemistry of Lutao andesites. *Acta Ocean. Taiwanica* **11**, 49–69 (1980).
37. Poreda, R. & Craig, H. Helium isotope ratios in circum-Pacific volcanic arcs. *Nature* **338**, 473–478 (1989).
38. Ono, S. *et al.* Measurement of a Doubly Substituted Methane Isotopologue, $^{13}CH_3D$, by Tunable Infrared Laser Direct Absorption Spectroscopy. *Anal. Chem.* **86**, 6487–6494 (2014).
39. Wang, D. T. *et al.* Nonequilibrium clumped isotope signals in microbial methane. *Science* **348**, 428–431 (2015).
40. Fiebig, J., Woodland, A. B., Spangenberg, J. & Oschmann, W. Natural evidence for rapid abiogenic hydrothermal generation of CH4. *Geochim. Cosmochim. Acta* **71**, 3028–3039 (2007).
41. Fiebig, J., Tassi, F., D'Alessandro, W., Vaselli, O. & Woodland, A. B. Carbon-bearing gas geothermometers for volcanic-hydrothermal systems. *Chem. Geol.* **351**, 66–75 (2013).
42. Douglas, P. M. J. *et al.* Methane clumped isotopes: Progress and potential for a new isotopic tracer. *Org. Geochem.* **113**, 262–282 (2017).
43. Etiope, G., Schoell, M. & Hosgörmez, H. Abiotic methane flux from the Chimaera seep and Tekirova ophiolites (Turkey): Understanding gas exhalation from low temperature serpentinization and implications for Mars. *Earth Planet. Sci. Lett.* **310**, 96–104 (2011).

44. Young, E. D. *et al.* The relative abundances of resolved (CH2D2)-C-12 and (CH3D)-C-13 and mechanisms controlling isotopic bond ordering in abiotic and biotic methane gases. *Geochim. Cosmochim. Acta* **203**, 235–264 (2017).
45. Abrajano, T. A. *et al.* Geochemistry of Reduced Gas Related to Serpentinization of the Zambales Ophiolite, Philippines. *Appl. Geochem.* **5**, 625–630 (1990).

Acknowledgments

The authors thank the Green Island Marine Research Station, Academia Sinica for the help on accommodation and sampling. We are appreciated for the help on sampling by Bing-Jye Wang, Yu-Chang Chang, and Hao Zheng. This research is supported by the National Natural Science Foundation of China (No. 41806051), the Aim for the Top University Program of Taiwan (03C0302), and Chinese Government Scholarship (201406325045).

Author Contributions

X.G.C. and C.T.A.C. conceived the idea and designed the work; X.G.C., P.S.L., and Y.Y. collected the samples; M.Z.Y., M.S., and S.O. analyzed the chemical and isotopic compositions of the samples; X.G.C., P.S.L., and Y.Y. interpreted the data; X.G.C., M.Z.Y., and C.T.A.C. wrote the manuscript. X.G.C. oversaw the overall structure of the manuscript as well as fieldwork and laboratory analysis. All authors reviewed the manuscript.

Competing interests: The authors declare no competing interests.

Figures and Figure legends

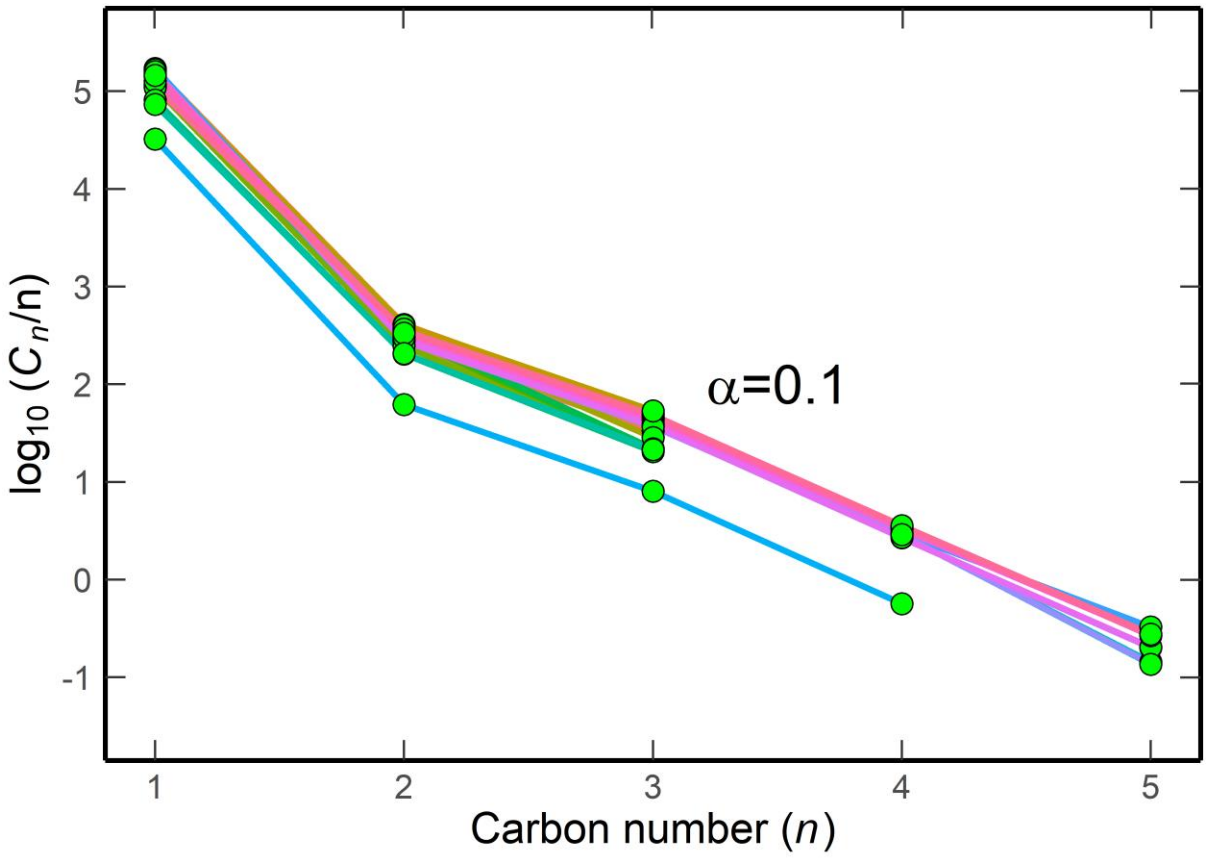

Fig. 1 Linear-log relationships between C_n/n (C_n is the concentration of hydrocarbon with carbon number n) and carbon number (n). α is the Andersen-Schulz-Flory distribution factor which was calculated as $\alpha = C_n/C_{n-1}$.

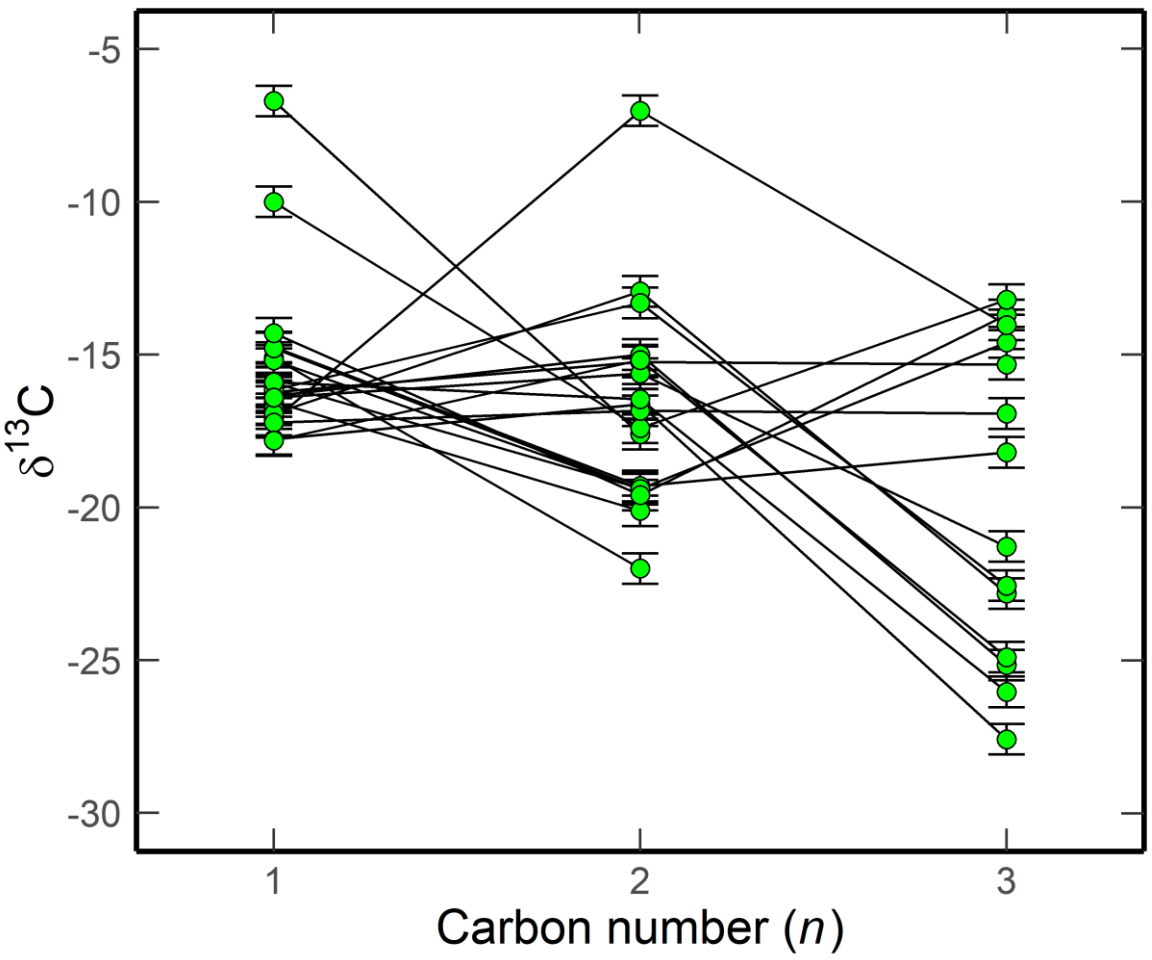

Fig. 2 Variation of $\delta^{13}C$ values (per mil, VPDB) with carbon number (*n*) for Lutao alkanes.

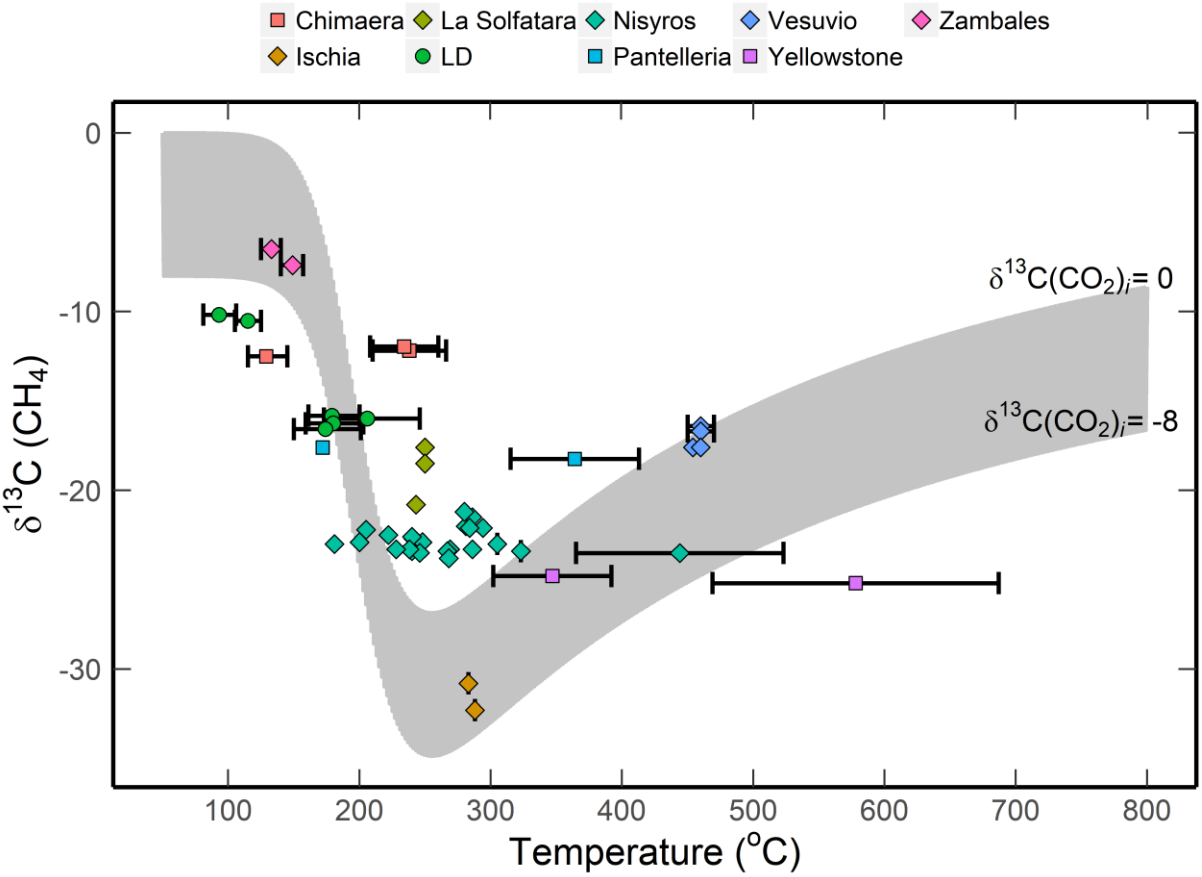

Fig. 3 Variation of $\delta^{13}C(CH_4)$ (‰ VPDB, gray area) at CH_4-CO_2 chemical/isotopic equilibrium as a function of temperature, assuming that CH_4 was totally derived from CO_2-H_2O fluids in a closed system. The modelling and calculations are shown in the Supplementary T3. Gas data from:

(1) LD: this study. Temperatures were calculated from methane isotopologue ($\Delta^{13}CH_3D$) abundances.

(2) Arc volcanic systems:

Nisyros, Pantelleria[40–42]: Temperatures were calculated from H_2-H_2O-CO-CO_2-CH_4 geoindicator or methane isotopologue ($\Delta^{13}CH_3D$ and $\Delta^{12}CH_2D_2$) abundances.

La Solfatara, Ischia, and Vesuvio [40,41]: Temperatures were calculated from H_2-H_2O-CO-CO_2-CH_4 geoindicator.

(3) Continental fields:

Chimaera [43,44]: Temperatures were estimated from methane isotopologue abundances.

Zambales Ophiolite [45]: Temperatures were calculated from H_2-H_2O equilibrium.

Yellowstone [42]: Temperatures were estimated from methane isotopologue abundances.

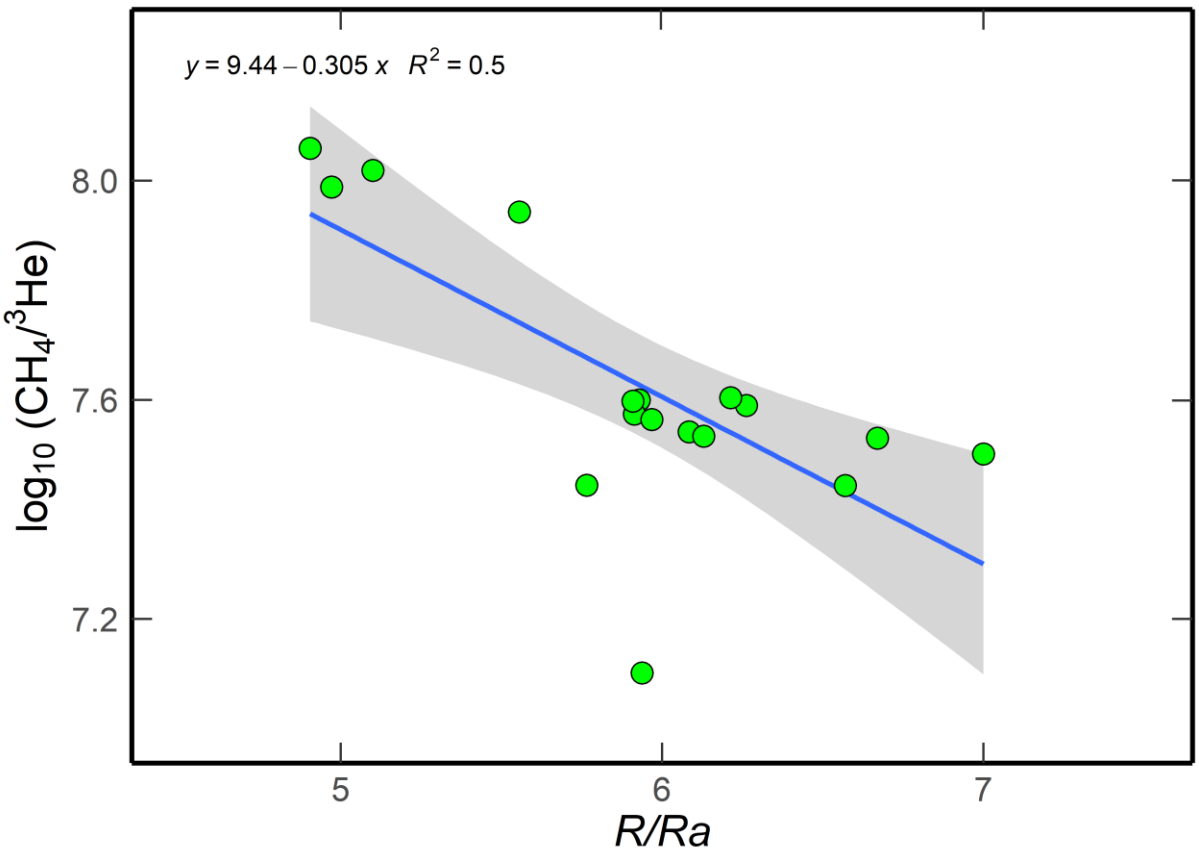

Fig. 4 Correlation between the R/R_a values and $\log_{10}(CH_4/^3He)$ values of Lutao gas samples. ^3He was used as a reference to indicate the relative CH_4 concentration because it was exclusively derived from the mantle. Most Lutao samples show $^4He/^{20}Ne$ ratios of dramatically higher than the air value (0.316). Therefore, air contribution was neglectable for Lutao helium, which was mixed from mantle-derived and crustal helium. The percentage of crustal contribution increases with decreasing R/R_a ratios [37].

Table 1 Stable carbon, radiocarbon, and hydrogen isotope data of gas discharges from the Lutao hydrothermal system. All isotope data are in ‰ units; $\delta^{13}C$ is reported as vPDB, δD as vSMOW.

Date	Sample	$\delta^{13}C$-CH_4	$\delta^{13}C$-CO_2	$\delta^{13}C$-C_2H_6	$\delta^{13}C$-C_3H_8	δD-CH_4	δD-C_2H_6	δD-C_3H_8
2012/5/5	012a1	-15.1	-13.4	-22.0				
2014/4/29	014a1	-15.9	-28.7	-19.4				
2014/4/29	014a2	-15.2	-23.8	-19.4				
2014/4/30	014a3	-16.5	-18.5	-20.1				
2014/9/22	014b1	-16.8	-21.7			-61	-74	
2014/9/22	014b3	-14.8	-17.5	-19.3	-18.2	-55	-88	
2014/9/22	014b4	-14.8	-13.1	-19.4	-14.6	-60	-86	
2014/9/22	014b5	-14.3	-14.9	-19.6	-13.7	-62	-85	
2014/9/23	014b6	-6.7	-19.1	-17.6		33	-61	
2014/9/23	014b7	-10.0	-18.0	-17.4	-13.2	-81	-93	
2016/5/20	016z1	-17.1	-14.0	-7.0	-14.0	-86	-180	-167
2016/5/20	016z3	-17.8	-14.6	-16.6	-27.6	-88	-179	-165
2016/5/20	016z4	-16.2	-15.2	-15.2	-15.3	-89	-180	-168
2016/5/21	016z5	-16.4	-14.3	-15.0	-25.2			
2016/5/21	016z6	-16.9	-10.3	-12.9	-22.8			
2016/5/21	016z7	-17.2	-13.7	-16.8	-16.9			
2016/5/21	016z8	-16.2	-10.1	-13.3	-22.6	-89	-183	-168
2016/5/22	016z9	-15.9	-8.3	-16.5	-26.0	-89	-185	-172
2016/5/22	016z10	-16.4	-10.9	-15.6	-21.3			
2016/5/22	016z11	-17.8	-9.3	-15.2	-24.9	-89	-170	-163
2018/10/30	018ZG6	-16.3				-78.8		
2018/10/30	018ZG10	-16.6				-80.5		

Measurement uncertainties:

$\delta^{13}C$: 2012-2016 samples, ±0.5‰; 2018 samples, ±0.2‰

δD: 2012-2014 samples, ±10‰; 2016 samples, ±2‰; 2018 samples, ±0.1‰

Table 2 Radiocarbon and methane isotopologue ($\Delta^{13}CH_3D$) abundances of Lutao methane.

Date	Sample	$\Delta^{13}CH_3D$	95% c.i.	Apparent T*	^{14}C-CH_4 (Fraction modern)
2016/5/20	016z1	2.38	±0.37	206+40/-33	
2016/5/21	016z5				<0.0044
2016/5/21	016z7				<0.0044
2016/5/22	016z10	2.68	±0.23	179+21/-18	
2018/10/30	018ZG6	2.67	±0.26	180+23/-21	
2018/10/30	018ZG10	2.74	±0.31	174+27/-24	
2018/10/30	018WG3[#]	3.61	±0.17	115±10	
2018/10/30	018WG4[#]	4.02	±0.25	93+13/-12	

* Apparent Temperature (^oC) was calculated using DFT model.

[#] Both samples were collected from the HWC vapor spring. The source of methane discharged from the HWC vapor spring was discussed in the Supplementary T4.